New Methods for Pyrolysis and Combustion Properties of Forest Litter: Enhanced Cone Calorimetry with Longleaf Pine Needles

Mark A. Dietenberger and **Charles R. Boardman**, USDA Forest Service, Forest Products Laboratory, Madison, Wisconsin;

and **David R. Weise**, USDA Forest Service, Pacific Southwest Research Station, Riverside, California

Abstract—New methods are sketched for determination of pyrolysis and combustion properties used in physical modeling of wildfires involving forest litter. The physical fire models, such as the Fire Dynamic Simulator, can benefit directly from detailed pyrolysis properties such as moisture isotherm properties of foliage; surface leaf emissivity varying with moisture content; foliage heat capacity varying from ambient temperature to 440 °C; dynamic moisture losses during direct heating; extractive volatiles profiling; and detailed pyrolysis kinetics. Although various instruments and methods for these properties are mentioned, this paper focuses on the pyrolysis and combustion properties associated with enhanced heat release rate calorimetry. Data from combustion tests of foliage litter on the specialized holder in the cone calorimeter, enhanced with water vapor flow and thermocouple measurements, are analyzed to provide ignition, chemical heat of combustion, mass losses, fire emissions, combustion efficiency, fuel elemental composition, and material interface temperatures as a function of time. Further, surface temperature measurements on heated leaf samples can be used to determine thermal conductivity as the thickness, density, heat capacity, and surface emissivity are independently measured. The methods presented here focus on longleaf pine (*Pinus palustris* Mill.) needles as a prominent litter component in the southeastern United States.

Keywords: combustion properties, forest litter properties, HRR calorimetry, pyrolysis kinetics

INTRODUCTION

There is a widely expressed need to improve upon the legacy pyrolysis and combustion properties of forest litter and live foliage developed two to three decades ago (e.g., Burgan and Susott 1991; Rothermel 1972; Sussott 1980, 1982; Shafizadeh et al. 1975, 1977) to adapt to the physical fire models (i.e., Fire Dynamic Simulator [FDS]), as well as accommodate the unusual properties of live and dead vegetation involved in wildfires that suggest improving the fire physics itself. Although the Forest Products Laboratory (FPL) in the Forest Service, Department of Agriculture has been developing pyrolysis and combustion properties for wood (Dietenberger 2002, 2012; Dietenberger and White 2001; Hagge et al. 2004; Tang and Eickner 1968), there have been occasions in which attention by FPL was devoted to vegetation in collaboration with other Forest Service scientists (Dibble et al. 2007; Dickinson et al. 2016; Safdari et al. 2018; White et al. 1996) as FPL acquired various equipment and expertise. Understanding live vegetation flammability properties has proved daunting in the recent past when using the various standard methods of measurements, such as the cone calorimeter in following ASTM E1354 (ASTM International 2017), or the various attempts at pyrolysis kinetics from measurements with thermal gravimetric analysis (TGA) (e.g., Bradbury et al. 1979; Sait et al. 2012; and many others).

In: Hood, Sharon; Drury, Stacy; Steelman, Toddi; Steffens, Ron, tech. eds. The fire continuum—preparing for the future of wildland fire: Proceedings of the Fire Continuum Conference. 21-24 May 2018, Missoula, MT. Proc. RMRS-P-78. Fort Collins, CO: U.S. Department of Agriculture, Forest Service, Rocky Mountain Research Station. 358 p.

These difficulties catalyzed a movement toward the nonstandard methods as with the Forced Ignition and Flame Spread Test (FIST) (McAllister and Weise 2016; McAllister et al. 2012), or with hot gases on single live leaves (Fletcher et al. 2007). We postulate that the methods used thus far have been unable to provide the basic properties requisite for accurate fire modeling. Recognition by the fire modeling community of fundamental differences between live and dead vegetation has recently resulted in a new physically based model of ignition for live fuels (Anand et al. 2017; Lamorlette et al. 2018).

Part of the problem is an inadequate description of the live leaf compositions, as from our recent summative analysis (for later publication) we know that hemicellulose, cellulose, and lignin make up only a majority of the dried mass of foliage, and that there are significant lipids, protein, fructose, glucose, pectin, and starch within the foliage. Further differences from the wood are noted, specifically that the foliage hemicellulose lacks the mannan that is significant in wood; the foliage cellulose is all amorphous but is mainly crystalline in wood; and lignin is simplified, thus indicating a new material to test for properties. This means the legacy vegetation properties that have been based on wood as a model material, such as the heat capacity and the moisture isotherm (Burgan 1988), are only first approximations, and should be updated to take advantage of modern measurement techniques. For example, modern differential scanning calorimeters (DSCs) with a modulation heating feature on top of a continuous heating rate can greatly improve the heat capacity value estimates and provide them as a function of temperature. With a similar heating profile applied to a homogenized sample, the testing can be done with TGA to normalize the mass of the degrading material so that heat capacity values can stay reasonable. This has recently been done at FPL for various shrub species native to the southeastern United States. All this preliminary work is complementary to the ultimate material testing in the enhanced cone calorimetry method, which overcomes the deficiencies in traditional standard testing in obtaining various thermal, moisture, pyrolysis, and combustion properties.

If leaves could hypothetically be described as very simple materials, such as the standard polymers, one could use solely the enhanced cone calorimeter measurements described herein, in conjunction with a computational fluid dynamics (CFD) model of pyrolysis and combustion, to derive the heat capacity, thermal conductivity, surface emissivity, ignition temperature, pyrolysis kinetics, heat of combustion (HOC), and emissions, via an advanced inverse method. These basic properties can then provide the CFD model with the ability to predict ignition time, fire intensity, fuel consumption, and smoke production as flammability indicators in various situations. However, the foliage is typically very hygroscopic and in fact made of several compounds, each having unique thermal, moisture, and flammability properties (Jolly et al. 2012, 2016). This complexity of the organic materials would certainly benefit from alternate instruments (apart from the cone calorimeter) specialized for measuring certain properties, such as heat capacity with the modulated DSC, surface emissivity with modified forward-looking infrared (FLIR) observations, and pyrolysis mass loss with high resolution TGA, that will be discussed in future papers. These additional data on properties would assist the use of enhanced cone calorimetry testing to determine difficult-to-obtain properties such as dynamic moisture loss, thermal conductivity, fuel pyrolysis, and HOC for intact material exposed to radiant and convective heat. By deriving these properties on a consistent leaf structure to directly incorporate into physical models, the modeling consisting of pyrolysis and combustion could then predict the flammability properties such as time to ignition, mass loss rates, heat release rates, and fuel consumptions, as tailored to the particular plant species. The known high variability of flammability between certain plant species may finally be explainable, and on a practical basis.

However, as the diffusion flame characteristics change with size, such that the production of carbon monoxide (CO) and soot do not scale (Dietenberger 2002), the chemical HOC (and also the combustion efficiency) is better determined with the larger basket fires of forest litter under the heat release rate (HRR) hood, rather than with the cone calorimeter. We note that the

enhanced cone calorimeter is incapable of measuring for radiant fraction, creeping flame spreading, or field emissions, as inputs to the CFD models. The properties derived for these flammability features require a larger diffusion flame, such as our basket tests of forest litter in a larger instrumented hood, which are not covered in depth in this paper. The other types of vegetation tested, but not discussed in detail in this paper, are 1) intact litter with oak (*Quercus* spp.) and maple (*Acer* spp.) on clay substrates for the cone calorimeter tests (Dickinson et al. 2016), 2) oak and maple litter in chickenwire baskets in HRR hood, and 3) various southeastern plant species for all the detailed measurements.

METHODS

Sample Preparation Approach

A local greenhouse of common species native to the southeastern United States was established to provide fresh leaves for testing. It was postulated that after a leaf is removed from the stem, it continues to undergo enzymatic hydrolysis (e.g., convert starch to sucrose, or protein to amino acids, or lipids to fatty acids) during air drying, which can negatively affect the determination of the live leaf moisture content. After experimentation, we found that the optimum drying regime for preserving live leaf properties meant heating the leaf in a vacuum oven at 45 °C. Under this drying regime the initial absorbed moisture evaporated quickly to prevent the hydrolysis modification of structural features. The leaf material was continuously exposed to a vacuum environment for several hours in order to completely evaporate the absorbed moisture that did not go into enzymatic hydrolysis. We found that for foliage with noticeably aromatic hydrocarbons (i.e., live longleaf pine [*Pinus palustris* Mill.] needles when plucked), the leaf material must be dried at temperatures much lower than the usual standard 105 °C, which is recommended for wood materials (ASTM D4442; ASTM International 2016). Indeed, 45 °C is a minimum temperature needed to avoid volatile loss while achieving a timely reasonable drying in a vacuum; it is the drying temperature in a vacuum used for standard material composition work at FPL. We recognize that there has been a longstanding discussion in the wildland fire community as to the appropriate temperature at which to dry biomass and live fuels in particular due to the presence of volatile and aromatic compounds.

Proper conditioning of the samples for further analysis included keeping them in a desiccator after vacuum drying to preserve the chlorophyll greenness, as it can also undergo enzymatic hydrolysis to a nitrogen-based acid when the leaf gains some moisture by exposure to the normal ambient humid air (typically found in a laboratory in Wisconsin, but also obviously relevant to other parts of the world). The samples were shipped in a very dry and oxygen-deprived sealed bag to commercial laboratories to prevent the leaf structure from degenerating into the various acids by hydrolysis or into carbon dioxide (CO_2) via cellular respiration.

By ensuring consistency among the samples as sourced from the live leaves, one can reduce significantly the errors related to the leaf structure degradations as described earlier. These consistent samples (by plucking a few mature leaves of a species to homogenize them and subject them to the same drying preservative method) then provided the basis for all other measurements that were needed on a dry basis with the added benefit of long shelf life for additional testing. However, there are tests that must be done on a live leaf basis, such as the solvent extraction for the lipid content (using hexane and isopropanol followed by acetone and water), and for flammability in the cone calorimeter and other fire tests of the foliage in the live state.

Our preliminary tests in the cone calorimeter at low irradiances showed a difference in pyrolysis mass loss, ignition, and combustion between the live leaf and an air-dried leaf. In companion work, Safdari et al. (2018) found differences in tar, gas, and char yields between live and dead (air dried for 1–2 weeks) samples of the same species that we are testing; however, there was no major difference in the composition of the chemical compounds observed. Indeed, our preliminary tests in the cone calorimeter at low irradiances show a difference in pyrolysis mass loss, ignition, and combustion between live leaves and leaves that have been air dried. Note that previously we outlined the process by which air-dried leaves undergo enzymatic hydrolysis of lipids, starch, and protein to simpler compounds that can then be easily pyrolyzed (with no charring) and thus more easily ignited. In contrast, the

live leaves have starch, protein, and other structures that stay relatively intact after rapid drying, making the leaves more resistant to mass loss, or a high heat of combustion, and ignition. We will now outline a new technique for examining leaf drying and volatile properties more closely using an enhanced cone calorimetry test method.

Enhanced Cone Calorimetry Method

As discussed earlier, the plants were grown in the local greenhouse. When a plant was selected for live testing, only the mature leaves were collected in a preweighed petri dish. A target weight of 3 grams was harvested (some plants have multiple leaves), the petri dish cover was put on, the petri dish plus sample was weighed, and the sample was delivered immediately (1–2 minutes) to the enhanced cone holder (fig. 1A) of the cone calorimeter.

In advance of the experiment, six 36-gauge Type-K thermocouples (T/Cs) were monitored to determine whether they were reading correctly and connected to the cone calorimeter data acquisition (DAQ) board. The bottom steel mesh was on the holder and three T/Cs were laid on it; small inert tape on the side kept them in place. The approximately 3 grams of leaves was removed from the petri dish and placed in a thin bunched layer on the steel mesh, taking care to ensure a leaf was placed over each T/C. The remaining three T/Cs were placed on top of the leaves. The top steel mesh was placed on top, and pressed and hooked to the bottom mesh to keep all the leaves flat so that they would receive the same irradiance (35 kW m^{-2} selected) from the cone's heater. In the case of longleaf needles, the typical trimmed lengths were limited by the diameter of the petri dish to 80 mm, and the typical 3 grams of needles provided approximately 3 layers of needles to adequately cover an area of 80 mm × 80 mm. The cone calorimeter itself was in waiting mode to begin the test at the selected irradiance. Using a FLIR to determine the surface temperatures proved inadequate. That is, by an independent method we determined that the fresh longleaf pine needles (LLPN) had an emissivity of 0.89 while the oven-dried LLPN had an emissivity of 0.68. This means that with a typical irradiance on the leaves of 35 kW m^{-2} the reflected radiation would cause significant errors to the FLIR surface temperature estimations, such that using thin T/Cs remains the more reliable temperature measure.

In addition to the standard gas analyzers for oxygen, CO_2, and CO in the FTT iCone® (Fire Testing Technology Ltd., East Grinstead, UK) calorimeter,

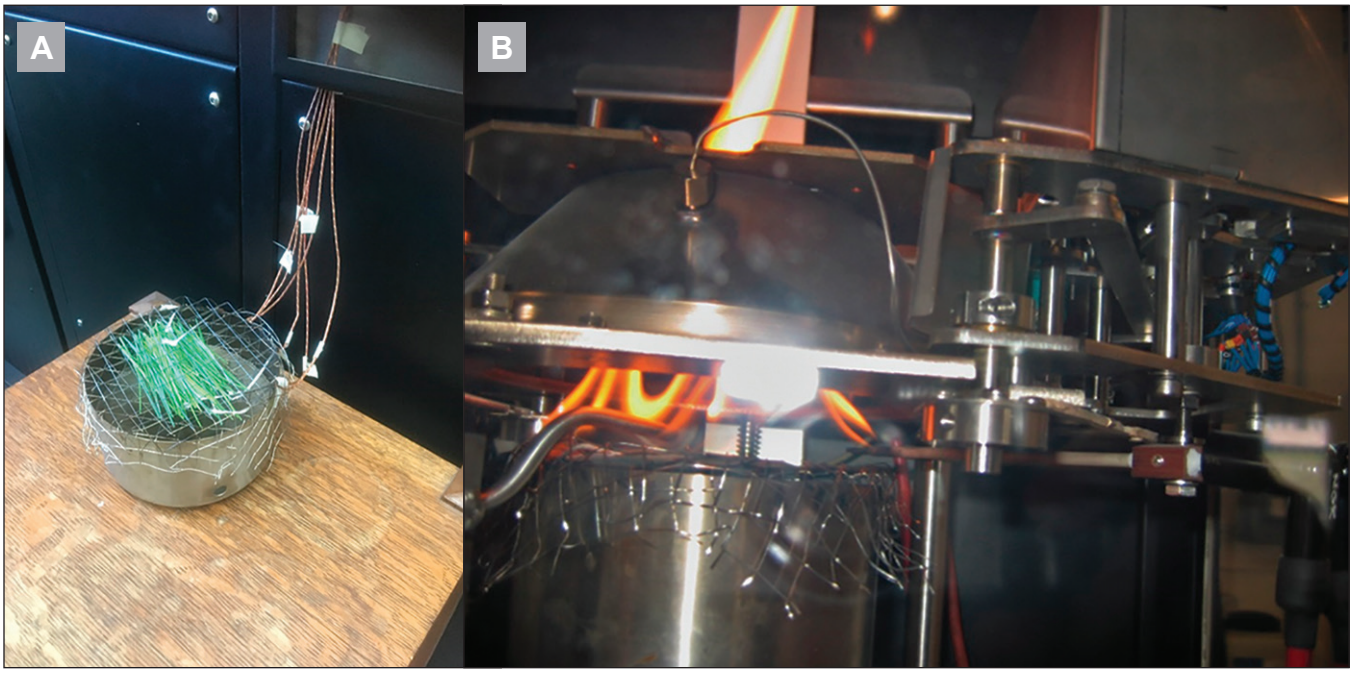

Figure 1—(A) New cone calorimeter holder with longleaf pine needles bedding constrained between wire grids, and (B) test specimen flaming as it is exposed to 35 kW m^{-2} in the cone calorimeter.

a Fourier Transform Infrared Radiation (FTIR) instrument and a fast-responding relative humidity (RH) in-line sensor (Sable RH 300; Sable Systems International, North Las Vegas, Nevada) have recently been added to the suite of instrumentation. The gas analyzers are calibrated by burning ethylene glycol instead of the usual methane. This is also helpful in the case of the RH sensor for getting the mass balance of all the gas measurements in agreement with the high accuracy weight cell mass loss, including the time responses for both delay and system dwell times. Considered along with these gas measurements is the soot extinction coefficient in the determination of the sample's "net" mass loss rate (MLR net), $\dot{m}_{net,fuel}$, via gas sampling as a comparison to weighed mass loss rate (MLR cell) in which the carbon, oxygen, and hydrogen mass flow rates provide the fuel mass flow rate as follows (Dietenberger 2012).

$$\dot{m}_{C,fuel} = \left(\frac{12}{44}\right)\dot{m}_{CO2} + \left(\frac{12}{28}\right)\dot{m}_{CO} + \dot{m}_{soot} \quad (1)$$

$$\dot{m}_{O,fuel} = \left(\frac{32}{44}\right)\dot{m}_{CO2} + \left(\frac{16}{28}\right)\dot{m}_{CO} + \left(\frac{16}{18}\right)\dot{m}_{H2O} - \Delta\,\dot{m}_{O2} \quad (2)$$

$$\dot{m}_{H,fuel} = \left(\frac{2}{18}\right)\dot{m}_{H2O} \quad (3)$$

$$\dot{m}_{net,fuel} = \dot{m}_{C,fuel} + \dot{m}_{O,fuel} + \dot{m}_{H,fuel} \quad (4)$$

The mass flow rates of oxygen, CO_2, and CO (grams second^{-1}) are provided as part of the standard equipment and the soot mass flow rate is calculated as the smoke production rate (SPR; extinction coefficient times volumetric flow rate) divided by the specific smoke area, as 8.3 m2 gram^{-1}. This in turn provides derivation of the volatile element composition (carbon, hydrogen, and oxygen) with time, as equations 1, 2, and 3 divided by equation 4. This easily translates to stoichiometric HOC with time (Dietenberger 2001) as:

$$HOC_{Stoich} = 13.23\left[\left(\frac{32\,\dot{m}_{C,fuel}}{12\,\dot{m}_{net,fuel}}\right) + \left(\frac{16\,\dot{m}_{H,fuel}}{2\,\dot{m}_{net,fuel}}\right) - \left(\frac{\dot{m}_{O,fuel}}{\dot{m}_{net,fuel}}\right)\right] \quad (5)$$

Chemical HOC due to inefficient diffusion flame combustion that produces CO and soot is determined as:

$$HOC_{chem} = HOC_{Stoich} - \left[\left(\frac{32.8\,\dot{m}_{C,fuel}}{\dot{m}_{net,fuel}}\right) + \left(\frac{10.1\,\dot{m}_{CO,fuel}}{\dot{m}_{net,fuel}}\right)\right] \quad (6)$$

In a typical experiment, the FTIR confirms that the major gases containing sulfur and nitrogen and the pure gaseous hydrocarbons are all in the parts per million range after flaming ignition, thereby improving the accuracy of equation 4 for the weight loss of the specimen. Combustion efficiency can be defined by the ratio of chemical heat of combustion to the stoichiometric heat of combustion. The other definition of combustion efficiency (Ward and Hao 1991) is also easily calculated as the moles of CO_2 divided by the combined moles of CO_2 , CO, and carbon (as soot). The spark igniter was adequate for igniting the LLPN sample after it was dried out. For some other species, an alternate pilot for igniting the white smoke after heating at the irradiance of 35 kW m^{-2} may be needed. The weigh scale is very sensitive, enough to measure the mass losses of 1-gram samples (although 3 grams was found more practical) to a small percentage error. Care must be taken to set the sample holder on and lighten the load of the six attached T/Cs with a tie to a frame to avoid a bias in the measured weight with time.

TEST RESULTS WITH FRESH LONGLEAF PINE NEEDLES

Temperature Profile of Sample

Three of the six thermocouples stayed adequately positioned and survived the test to measure the temperature as a function of time for differing depths (fig. 2). The temperature profile underneath the live needles gradually reached boiling temperature near 100 °C at 20 seconds, and was held nearly level until the point of ignition at 63 seconds. Exposed surface ignition temperature was 263 °C and the corresponding unexposed temperature was 138 °C, indicating a strong role for extractives and digestible material that pyrolyze at these temperatures in providing the volatile fuel for flaming combustion.

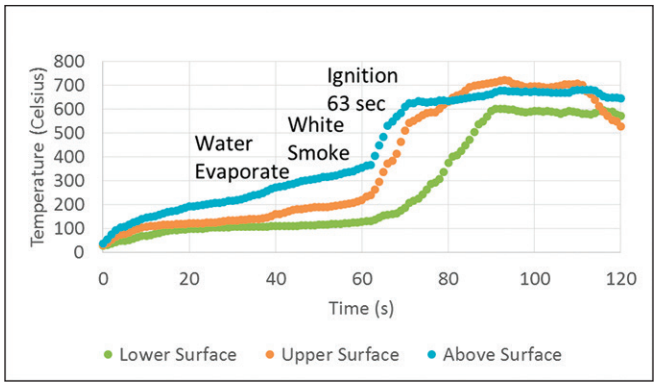

Figure 2—Temperatures measured temperatures by thermocouples on longleaf pine needles bedding on sample holder.

Our findings are similar to Susott's (1980, 1982) experiments using the catalytic oxidation feature of the evolved gas analyzer (EGA) with TGA on 5 mg of homogenized freeze-dried foliage to show the presence of extractives during pyrolysis at less than 200 °C, but which we also show with the 3.44 grams of intact live foliage. Although the exposed needles had temperature rapidly rising to 100 °C, and even rising to 200 °C prior to ignition, the temperature rise of the exposed needles was evidently constrained by the continuing water evaporation from the unexposed needles underneath the exposed needles until ignition. The delayed moisture effect has also been observed by Fletcher et al. (2007), but the effects on delayed temperature rise were observed for the first time in the current tests. Although also modeled (Shotorban et al. 2018; Yashwanth et al. 2016), the continuing refinement with the modeling will be possible with the current measurements. After ignition, the exposed needles had temperatures rapidly rising at rates of approximately 2100 °C minute^{-1}, while the unexposed and dried needles had a more delayed temperature rise due to the insulation by the exposed needles from the irradiance. The leveling out at 600 °C at 90 seconds as shown in figure 2 would be an indication that glowing combustion has been reached.

Various Mass Losses of Sample with Time

In figure 3, four significant mass losses are provided as a function of time. Of greatest relevance to pyrolysis modeling is the measured mass loss consisting of both water and the fuel. In an independent drying measurement with the vacuum oven, the moisture content is 65.7 percent green basis (192 percent dry basis), which also corresponds to total water mass loss prior to ignition in figure 3. The calculation of water vapor mass flow rate involves multiplying the water vapor mass fraction of the pyrolysis/combustion products (i.e., the increment in RH values with the in-line sensor) with the measured air exhaust mass flow rate. It is seen that the measured water vapor mass flow rate is in agreement with the measured weight loss rate in the period up to about 60 seconds after the irradiant exposure, as would be expected before ignition. After ignition, the water vapor mass flow rate is then primarily from the combustion of fuel with hydrogen composition, as the moisture content has been depleted at the point of ignition prior to ignition. The stoichiometric oxygen consumption mass rate is shown as heat release rate (as product of equations 4 and 5) divided by 13.23 (heat of combustion per mass of oxygen consumed in kJ gram^{-1}). The HRR peaking at 68 seconds corresponds to a surface temperature of 414 °C and backside temperature of 165 °C, which is much higher than what Susott (1982) observed with EGA/TGA of 5 mg of foliage heated at the very slow rate of 20 °C minute^{-1}. This would be a predicted effect of Arrhenius pyrolysis kinetics, in which the increasing of the heating rate corresponds to shifting the peak pyrolysis rates to occur at higher temperatures. Given the high rate of heating (2100 °C minute^{-1}) of the sample in the cone calorimeter test, it is then imperative to use tiny T/Cs in contact with the surfaces (unlike that in the TGA) to reflect the best accuracies with the temperature values during pyrolysis. Not shown is the similar profile of CO_2 and CO. As can be seen in figure 3, the weigh cell had an "extraneous bump" for the first few seconds while the makeshift radiant shutter was removed (the cone's shutter was inoperative so a manual shutter with a steel plate was devised).

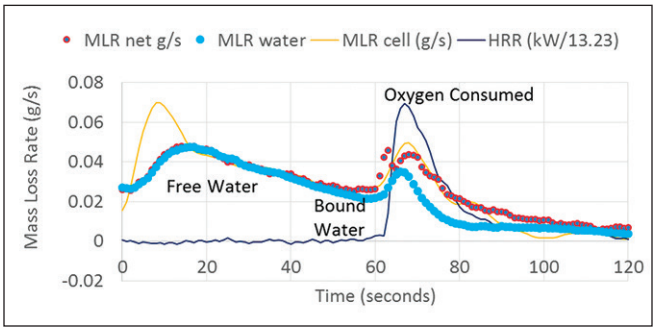

Figure 3—Mass loss rates (MLRs) for weigh cell, water, fuel, and oxygen during longleaf pine needle testing at 35 kW m^{-2}. HRR: heat release rate.

Major Combustion Emissions with Time

Four major emissions products common to all organic diffusion fires, CO_2, CO, water (H_2O), and soot, are provided as a function of time in figure 4. Emissions are calculated as the mass flow rates of CO_2, CO, H_2O, and soot divided by net mass loss rate (MLR), and therefore are dynamic emission measures. Obviously water is the major emission prior to ignition due to the live LLPN water evaporation, while the white smoke from the combustible volatiles (Yokelson et al. 1997)

started to appear at 40 seconds at above 159 °C, as separate from that of the moisture. Byram (1959) calculated that the initial fuel moisture made up most of the water vapor produced in the combustion reaction when moisture content of the fuel (dry weight basis) exceeded 56 percent. This is only applicable to the green fuel as a whole, corresponding to the full 120 seconds of the current test, and provides an adequate approximation for wood stove or furnace application.

However, in a previous discussion, we determined that all of the fuel moisture in the cone calorimeter test with the thin leaf bedding has evaporated prior to ignition, at least for the LLPN, and that the water vapor after the ignition event is sourced entirely from the chemical hydrogen of the dried decomposing fuel. This provides an additional pyrolysis and combustion detail that was not available for the Byram combustion calculations. The white smoke emission measured by the laser smoke system (but not detected by the FTIR for the simpler compositions) is really about double that shown in figure 4 as the white smoke specific extinction area is about half that of black smoke ($4.4\ m^2\ gram^{-1}$ in Grexa et al. 2012). However, the black smoke is more important to measure than the white smoke for deriving the heat of combustion. It is seen that the CO emissions have quite low values during drying and flaming, until at the time of 80 seconds the CO mass fraction of the fuel undergoing pyrolysis reaches 0.16 while the H_2O emissions drop to 0.4, indicating the onset of glowing combustion. By 90 seconds, the sample mass was so small that errors begin creeping in, such as transient ambient RH that is responsible for the extraneous higher water vapor mass fraction at the end of the test.

Fuel Elemental Composition with Time

The trace gas emissions measured with the FTIR showed that the compounds containing sulfur and nitrogen and also the hydrocarbons were in the parts per million range, leaving the oxygen consumed, the CO_2, H_2O, and CO gases produced, and soot as solid carbon as the major measured compounds. It was possible to derive the combusting fuel elemental composition of carbon, oxygen, and hydrogen in these compounds as varying with time (equations 1, 2, and 3 divided by equation 4). We assume the initial volatile mass production is merely the water with zero carbon fraction, with hydrogen mass fraction as 0.11, and oxygen mass fraction as 0.88. Recall that figure 3 showed a small amount of volatiles in comparison to the water vapor prior to ignition. However, the white smoke as measured by the laser extinction was roughly approximated as solid carbon and is represented in figure 5 as an increasing carbon fraction while the oxygen and hydrogen fractions are decreasing. Upon volatile ignition at 63 seconds, the white smoke is converted to CO_2, H_2O, CO, and black smoke. It is evident that the leaf volatiles begin with oxygenated hydrocarbons as sourced from the extractives and digestible compounds, as indicated by carbon and hydrogen fractions (solid lines) being higher than that of reference sugar (dashed lines) and the oxygen fraction (solid line) as being lower than that of the reference sugar (dashed line).

The volatile composition then proceeded to the tar elemental compositions of carbon, oxygen, and hydrogen close to that of glucose by 80 seconds. The combusting fuel after that becomes more of solid char surface oxidation, along with the diminishing volatiles,

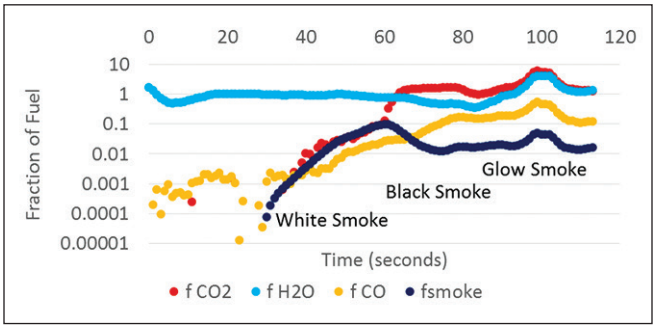

Figure 4—Major emissions of longleaf pine needles bedding during pyrolysis and combustion.

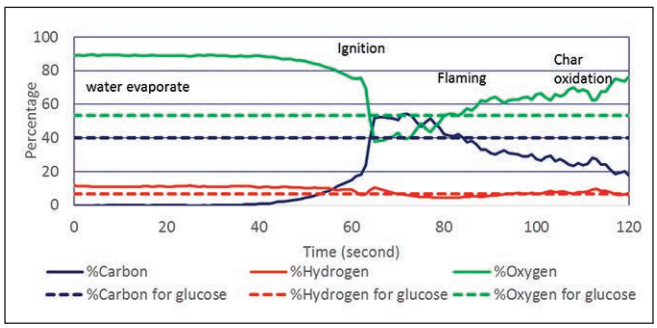

Figure 5—Estimated elemental composition of the devolved fuel for longleaf pine needles.

such that by the time of 90 seconds, the remaining mass is so small that it leads to increasing errors for the derived elemental composition of combusting fuel. We note that by integrating the fuel elemental composition over time, one can derive approximately the original dried fuel composition as the formula $C_6H_{11.7}O_{5.3}$. Then the elemental composition of the noncombusting fuel residue can be determined as a function of time by subtracting the combusting fuel composition from the original fuel composition.

Heat of Combustion Measures with Time

The availability of the combusting fuel elemental composition with time means that the stoichiometric oxygen mass consumption per fuel mass is easily calculated as a function of time. The stoichiometric HOC was estimated accurately from equation 5. It is shown in figure 6 as the upper red line starting at 40 seconds, which was when the laser extinction system began sensing white smoke. The reliability for the HOC value as measured in the cone calorimeter during flaming conditions can be assessed by comparing to the corresponding oxygen bomb measurement for the net HOC for vacuum-dried LLPN on the dry basis as the value, 19 kJ gram^{-1}. An independent gas chromatography/mass spectrometry measurement of the extractives for various lipid type compounds (e.g., terpenoids, oils, fatty acid) were found with the OH groups attached in varying amounts. This result indicates the good degree of reliability for the net heat of combustion starting at 24 kJ gram^{-1} at 65 seconds and decreasing monotonically as would be expected with the sequence of digestible material (protein has 23.6 kJ gram^{-1} for gross HOC), carbohydrates (glucose has 14 kJ gram^{-1} for net HOC), and charring lignin

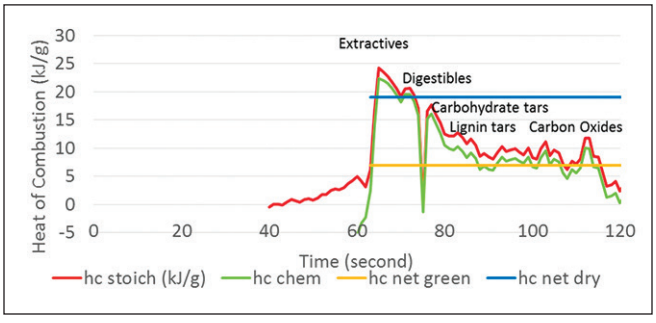

Figure 6—Heats of combustion (HCs; stoich = stoichiometric; chem = chemical) for the fresh longleaf pine litter exposed to 35 kW m^{-2}.

pyrolysis as the material temperatures continue to rise to at least 600 °C. Note that the wet basis net HOC based on the oxygen bomb calorimeter is 7 kJ gram^{-1}, indicating the serious effect of the leaf moisture content on its flammability. Also shown in figure 6 is the calculated chemical HOC due to the incomplete combustion of the diffusion flames that resulted in CO and soot as emissions.

DISCUSSION AND CONCLUSIONS

Implications for Thermal and Moisture Properties

Some of the properties can fortunately be determined independently and perhaps better with other equipment. For example, surface emissivity of the leaves was determined with the enhanced FLIR method, the heat capacity on dried basis as a function of temperature with the modern modulated DSC, moisture characteristics with the water activity meter, and the moisture/pyrolysis kinetics with the high resolution TGA, particularly with the foliage chemistry providing various compositions. However, the thermal conductivity cannot be determined in an independent apparatus because of the rough and thin surfaces of the leaves. Further, the thermal conductivity is very dependent on the internal construction of the leaves, meaning that the samples must be intact and layered thinly. As a demonstration concerning thermal conductivity, the temperature profiles in figure 2 suggest a rough estimation for thermal conductivity as follows. The surface equilibrium temperature of the exposed surface at 100 seconds is measured at 696 °C, which provides an estimation for the effective heat transfer coefficient of the material cooling to the environment from the equation:

$$\varepsilon_s q_r = \varepsilon_s \sigma (T_{eq}^4 - T_a^4) + h_c (T_{eq} - T_a) = h_{eff} (T_{eq} - T_a) \quad (7)$$

The point of ignition at 63 seconds in figure 2 provides a quasi-steady temperature spot in which the LLPN has just dried out and the heat being absorbed by heat capacity and water evaporation is at a minimum, leading to conductive heat losses into the triple-layered LLPN bed approximated with the equation:

$$\varepsilon_s q_r \sim h_{eff} (T_{ig} - T_a) + k (T_{ig} - T_{back}) / \delta \quad (8)$$

Using the previously mentioned values of temperatures, irradiance, and surface emissivity and with the three-layered thickness measured at $\delta = 0.85$ mm, the thermal conductivity, k, is calculated to be 0.1 W m^{-1} K^{-1}, which is often the value reported for wood in the literature. Obviously, the use of a CFD pyrolysis model can offer more refined estimation of thermal conductivity that should also include dependence on temperature and moisture content.

The moisture evaporation is also dependent on the internal construction of the leaf, as the surface layers have a cuticle composed of a waxy substance primarily composed of very long-chain fatty acids and stomata to control moisture transport to the environment (Raven et al. 1981; Yeats and Rose 2013). The material properties of heat capacity, thermal conductivity, and surface emissivity are strong functions of the moisture content. Although there are several CFD models to predict a material's thermal and moisture time responses, the profiles provided in figures 2 and 3 will challenge those models, to where perhaps only a few will succeed in predicting the profiles, or be a cause for introducing new physics in the pyrolysis model.

Implications for Pyrolysis and Combustion Properties

The foliage chemistry (methods to be discussed in another paper) for fresh LLPN litter indicates significant compositions of lipids, protein, glucose, fructose, starch, and pectin with a corresponding decrease in the celluloses in comparison to wood, while the lignin content remained similar to wood (table 1). Therefore, for the compositions aside from the lignin, there is expected to be no or minimal charring during the pyrolysis event, indicating the effective use of the TGA mass loss for the vacuum-dried leaf to define the pyrolysis kinetics of the corresponding compositions and to provide estimations for their volatile elemental composition and the corresponding stoichiometric HOC. However, the difficulties of pyrolysis in the cone calorimeter experiments include extremely high heating rates and temperature profiles existing within the thin leaf that may scuttle any attempts at a thermally thin formulation for the apparently very thin leaves. If the moisture and pyrolysis kinetics are coupled with a CFD model of heat and moisture flow, the challenge will be to reproduce the measured profiles in figures 2 to 6 with a reasonable set of properties that would allow the pyrolysis model to adapt to a variety of fire scenarios.

Table 1—Composition of fresh longleaf pine litter.

Component	Dry basis (%)
Extract (lipids)	22.3
Protein	7.4
Glucose	1.4
Fructose	0.8
Pectin	2.1
Hemicellulose	15.0
Cellulose	19.0
Starch	0.7
Lignin	26.6
Minerals	2.0
Silicates	0.6
Total	97.9
Moisture - dry basis	191.6

Concluding Remarks

In this paper we reported on fresh LLPN as a difficult material for which to derive thermal and moisture properties, and also on pyrolysis and combustion properties with an enhanced cone calorimetry test method involving a new sample holder design, attachment of T/Cs to the sample surfaces, and added gas sensors for H_2O and the FTIR. The dynamically changing profiles of various simultaneous measurements along with the complexity of the foliage material make determination of any one parameter in isolation to be difficult. Despite this difficulty, it was interesting that there were quasi-steady portions of the exposed and backside temperatures in the cone calorimeter test that provided a rough estimation of the thermal conductivity of LLPN at the point of ignition. Using a CFD model to refine the estimates of the thermal conductivity would be an improvement, particularly in that new nonstandard techniques

were developed for determining other parameters such as surface emissivity and heat capacity as a function of temperature and moisture content, along with the independent physical measurements of leaf thicknesses and density. It is now possible to create detailed pyrolysis kinetics models based on a recently completed detailed profiling of dried foliage composition for extractives, protein, fructose, glucose, pectin, hemicellulose, cellulose, starch, lignin, and minerals. Data from high resolution TGA and enhanced cone calorimeter tests are being analyzed to provide an alternative to the relatively simple pyrolysis kinetics currently used in FDS. This would imply new fire physics modeling capability to be added to FDS and other CFD models. Such enhancements are expected to improve prediction of foliage degradations and combustions subjected to varying environments while providing greater speed, accuracy, and flexibility to the numerical schemes.

ACKNOWLEDGMENTS

This work was partially supported by the DOD/EPA/DOE Strategic Environmental Research and Development Program project RC-2640. We thank the staff of FPL for their support of this work. This manuscript was prepared by Federal government employees as a part of their official duties and is therefore in the public domain and not subject to copyright.

REFERENCES

Anand, C.; Shotorban, B.; Mahalingam, S.; [et al.]. 2017. Physics-based modeling of live wildland fuel ignition experiments in the forced ignition and flame spread test apparatus. Combustion Science and Technology. 189: 1551–1570.

ASTM International. 2016. ASTM D4442 – 16: Standard test methods for direct moisture content measurement of wood and wood-based materials. West Conshohocken, PA. Available at https://www.astm.org/Standards/D4442.htm.

ASTM International. 2017. ASTM E1354: Standard test method for heat and visible smoke release rates for materials and products using an oxygen consumption calorimeter. West Conshohocken, PA. Available at https://www.astm.org/Standards/E1354.htm.

Bradbury, Allan G.W.; Sakai, Yoshio; Shafizadeh, Fred. 1979. A kinetic model for pyrolysis of cellulose. Journal of Applied Polymer Science. 23: 3271–3280.

Burgan, Robert E. 1988. 1988 revisions to the 1978 National Fire-Danger Rating System. Res. Pap. SE-273. Asheville, NC: U.S. Department of Agriculture, Forest Service, Southeastern Forest Experiment Station. 39 p.

Burgan, R.E.; Susott, R.A. 1991 Influence of sample processing techniques and seasonal variation on quantities of volatile compounds of gallberry, saw-palmetto, and wax myrtle. International Journal of Wildland Fire. l: 57–62.

Byram, George M. 1959. Combustion of forest fuels. In: Davis, Kenneth P., ed. Forest fire: Control and use. 1st ed. American Forestry Series. New York: McGraw-Hill: 61–89.

Dibble, Alison C.; White, Robert H.; Lebow, Patricia K. 2007. Combustion characteristics of north-eastern USA vegetation tested in the cone calorimeter: Invasive versus non-invasive plants. International Journal of Wildland Fire. 16: 426–443.

Dickinson, Matthew B.; Hutchinson, Todd F.; Dietenberger, Mark; [et al.]. 2016. Litter species composition and topographic effects on fuels and modeled fire behavior in an oak-hickory forest in the eastern USA. PLOS ONE. 11: e0159997.

Dietenberger, Mark. 2002. Update for combustion properties of wood components. Fire and Materials Journal. 26: 255–267.

Dietenberger, Mark. 2012. Pyrolysis kinetics and combustion of thin wood by an advanced cone calorimetry test method. Journal of Thermal Analysis and Calorimetry. 109: 1215–1228.

Dietenberger, Mark A.; White, Robert H. 2001. Reaction-to-fire testing and modeling for wood products. In: Proceedings, 12th Annual BCC conference on flame retardancy; 2001 May 21–23; Stamford, CT. Norwalk, CT: Business Communications Co.: 54–69.

Fletcher, Thomas H.; Pickett, Brent M.; Smith, Steven G.; [et al.]. 2007. Effects of moisture on ignition behavior of moist California chaparral and Utah leaves. Combustion Science and Technology. 179: 1183–1203.

Grexa, Ondrej; Dietenberger, Mark A.; White, Robert H. 2012. Reaction-to-fire of wood products and other building materials. Part 1: Room/Corner test performance. Res. Pap. FPL-RP-663. Madison, WI: U.S. Department of Agriculture, Forest Service, Forest Products Laboratory. 51 p.

Hagge, Matthew J.; Bryden, Kenneth M.; Dietenberger, Mark A. 2004. Effects of backing board materials on wood combustion performance. Proceedings, Wood & fire safety: 5th International scientific conference; 2004 April 18–22; High Tatras, Slovakia. Zvolen, Slovak Republic: Technical University of Zvolen, Faculty of Wood Science and Technology: 51–58.

Jolly, W. Matt; Hintz, John; Linn, Rodman L.; [et al.]. 2016. Seasonal variations in red pine (*Pinus resinosa*) and jack pine (*Pinus banksiana*) foliar physio-chemistry and their potential influence on stand-scale wildland fire behavior. Forest Ecology and Management. 373: 167–178.

Jolly, W. Matt; Parsons, Russell A.; Hadlow, Ann M.; [et al.]. 2012. Relationships between moisture, chemistry, and ignition of *Pinus contorta* needles during the early stages of mountain pine beetle attack, Forest Ecology and Management. 269: 52–59.

Lamorlette, A.; El Houssami, M.; Morvan, D. 2018. An improved non-equilibrium model for the ignition of living fuel. International Journal of Wildland Fire. 27: 29–41.

McAllister, S.; Grenfell, I.; Hadlow, A.; [et al.]. 2012. Piloted ignition of live forest fuels. Fire Safety Journal. 51: 133–142.

McAllister, S.; Weise, D.R. 2016. Effects of season on ignition of live wildland fuels using the FIST apparatus. Combustion Science and Technology. 189: 231–247.

Raven, Peter H.; Evert, Ray F.; Curtis, Helena. 1981. Biology of plants. 3rd ed. New York: Worth Publishers.

Rothermel, Richard C. 1972. A mathematical model for predicting fire spread in wildland fuels. Res. Pap. INT-RP-115. Ogden, UT: U.S. Department of Agriculture, Forest Service, Intermountain Forest and Range Experiment Station. 40 p.

Safdari, Mohammad-Saeed; Rahmati, Mahmood; Amini, Elham; [et al.]. 2018, Characterization of pyrolysis products from fast pyrolysis of live and dead vegetation native to the southern United States. Fuel. 229: 151–166.

Sait, Hani; Hussain, Ahmad; Salema, Arshad Adam.; Ani, Farid Nasir. 2012. Pyrolysis and combustion kinetics of date palm biomass using thermogravimetric analysis. Bioresource Technology. 118: 382–389.

Shafizadeh, F.; Chin, P.S.; Degroot, W.F. 1975. Mechanistic evaluation of flame retardants. Journal of Fire & Flammability/Fire Retardant Chemistry Supplement. 2: 195–203.

Shafizadeh, F.; Chin, P.S.; DeGroot, W.F. 1977. Effective heat content of green forest fuels. Forest Science. 23: 81–89.

Shotorban, Babak; Yashwanth, Banglore L.; Mahalingam, Shankar; Haring, Dakota J. 2018. An investigation of pyrolysis and ignition of moist leaf-like fuel subject to convective heating. Combustion and Flame. 190: 25–35.

Susott, Ronald A. 1980. Thermal behavior of conifer needle extractives. Forest Science. 26: 347–360.

Susott, Ronald A. 1982. Characterization of thermal properties of forest fuels by combustible gas analysis. Forest Science. 28: 404–420.

Susott, R.A.; F. Shafizadeh, and T.W. Aanerud. 1979. A quantitative thermal analysis technique for combustible gas detection. Journal of Fire and Flammability 10: 94–104.

Tang, Walter K.; Eickner, Herbert W. 1968. Effect of inorganic salts on pyrolysis of wood, cellulose, and lignin determined by differential thermal analysis. Res. Pap. FPL-82. Madison, WI: U.S. Department of Agriculture, Forest Service, Forest Products Laboratory. 29 p.

Ward, Darold E.; Hao, Weimin. 1991. Projections of emissions from burning of biomass for use in studies of global climate and atmospheric chemistry. Paper 91-128.4 presented at the 84th annual meeting and exhibition of the Air and Waste Management Association; 1991 June 16–21; Vancouver, BC. Available at http://www.treesearch.fs.fed.us/pubs/43258.

White, Robert H.; Weise, David R.; Frommer, Susan. 1996. Preliminary evaluation of the flammability of native and ornamental plants with the cone calorimeter. In: Proceedings, 21st international conference on fire safety; 1996 January 8–12; Millbrae, CA: 256–265.

Yashwanth, B.L.; Shotorban, B.; Mahalingam, S.; [et al.]. 2016. A numerical investigation of the influence of radiation and moisture content on pyrolysis and ignition of a leaf-like fuel element. Combustion and Flame. 163: 301–316.

Yeats, Trevor H.; Rose, Jocelyn K.C. 2013. The formation and function of plant cuticles. Plant Physiology. 163: 5–20.

Yokelson, Robert J.; Susott, Ronald; Ward, Darold E.; [et al.]. 1997. Emissions from smoldering combustion of biomass measured by open-path Fourier Transform Infrared spectroscopy. Journal of Geophysical Research: Atmospheres. 102: 18865–18877.